Detection and Characterization of CD8$^+$ Autoreactive Memory Stem T Cells in Patients With Type 1 Diabetes

Debora Vignali,[1] Elisa Cantarelli,[1] Carlotta Bordignon,[1] Adriana Canu,[1] Antonio Citro,[1] Andrea Annoni,[2] Lorenzo Piemonti,[1] and Paolo Monti[1]

Diabetes 2018;67:936–945 | https://doi.org/10.2337/db17-1390

Stem memory T cells (Tscm) constitute the earliest developmental stage of memory T cells, displaying stem cell–like properties, such as self-renewal capacity. Their superior immune reconstitution potential has sparked interest in cancer immune therapy, vaccine development, and immune reconstitution, whereas their role in autoimmunity is largely unexplored. Here we show that autoreactive CD8$^+$ Tscm specific for β-cell antigens GAD65, insulin, and IGRP are present in patients with type 1 diabetes (T1D). In vitro, the generation of autoreactive Tscm from naive precursors required the presence of the homeostatic cytokine interleukin-7 (IL-7). IL-7 promotes glucose uptake via overexpression of GLUT1 and upregulation of the glycolytic enzyme hexokinase 2. Even though metabolism depends on glucose uptake, the subsequent oxidation of pyruvate in the mitochondria was necessary for Tscm generation from naive precursors. In patients with T1D, high expression of GLUT1 was a hallmark of circulating Tscm, and targeting glucose uptake via GLUT1 using the selective inhibitor WZB117 resulted in inhibition of Tscm generation and expansion. Our results suggest that autoreactive Tscm are present in patients with T1D and can be selectively targeted by inhibition of glucose metabolism.

Long-lived memory T cells are generated during an immune response and persist in the host for a rapid and enhanced response after a subsequent encounter with the antigen. The memory compartment is composed by different T-cell subsets, conventionally divided into central memory (Tcm), effector memory (Tem), and CD45RA$^+$ effector memory (Temra) according to their phenotype, gene expression, and anatomical localization (1). These memory T-cell subsets are characterized by a rapid turnover, with half-lives of a few months (2). The existence of a long-lived memory precursor with stem cell–like properties (stem memory T cells [Tscm]) was first hypothesized and subsequently described in mice (3), nonhuman primates (4), and humans (5). Tscm display a CD45RA$^+$CCR7$^+$CD95$^+$ phenotype, are long-lived and self-renewing, and have an extraordinary capacity to expand in a robust effector progeny. Tscm can play a role in the pathogenesis of autoimmune diseases, in which they can serve as a reservoir of autoreactive effector T cells to sustain chronic destruction of targeted tissues (6).

Type 1 diabetes (T1D) results from a chronic autoimmune destruction of insulin-producing β-cells mediated by autoreactive T cells. Several β-cell autoantigens are targets of autoimmunity. Of these, GAD65, (pro)insulin, and islet-specific glucose-6-phosphatase catalytic subunit–related protein (IGRP) appear to be highly antigenic in humans (7). Some characteristics of the autoreactive T-cell response in patients with T1D lead us to hypothesize that autoreactive Tscm can be generated during the pathogenesis of the disease. Three observations were key. First, although T cells specific for β-cell autoantigens are commonly found in subjects with no other sign of autoimmunity (8), only patients with T1D autoreactive T cells show features of antigen experience, including the expression of memory markers, reduced telomere length (9), and activation in the absence of costimulation (10). Second, generation and maintenance of T-cell autoimmunity in T1D involves the homeostatic cytokine interleukin 7 (IL-7) (11), which was also shown to provide essential signals for the generation of Tscm from naive precursors (12). Third, memory autoimmunity is long lasting, as testified in patients with T1D

[1]San Raffaele Diabetes Research Institute, IRCCS San Raffaele Scientific Institute, Milan, Italy
[2]San Raffaele Telethon Institute for Gene Therapy, IRCCS San Raffaele Scientific Institute, Milan, Italy
Corresponding author: Paolo Monti, monti.paolo@hsr.it.

Received 17 November 2017 and accepted 23 February 2018.
This article contains Supplementary Data online at http://diabetes.diabetesjournals.org/lookup/suppl/doi:10.2337/db17-1390/-/DC1.

receiving pancreas and islet allografts years after the onset of the disease, which, despite strong immunosuppression, is frequently associated with autoimmunity recurrence (13). The autoreactive memory T-cell response is difficult to control with standard immune modulation and immune suppression (14–16). Also, more aggressive procedures based on profound T-cell depletion showed a high frequency of autoimmunity relapse (17). In this context, a selective deletion of autoreactive Tscm clones could represent an unexplored and promising approach to permanently delete the autoreactive T-cell response.

In this study, we evaluated the presence of $CD8^+$ Tscm specific for β-cell autoantigens GAD65, insulin, and IGRP in patients with T1D and subjects with no sign of autoimmunity. Further, we investigated the generation of autoreactive Tscm from naive precursors in order to identify potential target pathways. The findings indicate that autoreactive Tscm are present in patients with T1D and provide evidence that Tscm can be targeted by inhibition of glucose metabolism.

RESEARCH DESIGN AND METHODS

Patients

Patients with long-standing T1D (LS-T1D; mean diabetes duration 27 ± 6 years) and recent-onset T1D (RO-T1D; <6 months) were recruited at the islet transplantation program at the IRCCS San Raffaele Scientific Institute. Blood samples were collected pretransplant. The protocols were approved by the ethical committee of the IRCCS Ospedale San Raffaele, and informed consent for the studies was obtained from patients. All subjects were selected for positivity for the HLA-A*0201 allele for antigen-specific T-cell detection with HLA-A*0201 peptide dextramers.

Detection of Antigen-Specific Tscm

Whole blood samples from patients with T1D and healthy control subjects were stained using the following monoclonal antibodies (mAbs): CD3 PE-Cy7 (clone SP34-2), CD4 Pacific Blue (clone RPA-T4), CD8 BV450 (clone SK1), CD45RA allophycocyanin (APC)-H7 (clone HI100), CD62L PE (clone 150503), and CD95 fluorescein isothiocyanate (FITC) (clone DX2; BD Biosciences, San Jose, CA). GLUT1 PerCP (clone 202915) was from R&D Systems. For antigen-specific T-cell detection, we used APC-labeled HLA-A*0201 dextramers from Immundex (Copenhagen, Denmark) (Supplementary Table 1). Zombie UV Fixable Viability Dye (BioLegend) was used to exclude dead cells. Cell debris and doublets were excluded on the basis of side versus forward scatter. Samples were acquired on a Becton Dickinson LSR-Fortessa X-20 with FACS Diva software and analyzed using FlowJo software version 9.3.2 (Tree Star). Telomere length was measured using FITC-conjugated peptide nucleic acid (PNA) probe (Dako) according to the manufacturer's instructions.

Clonal Capacity

Clonal capacity was defined as the capacity of a single cell to expand under antigen-specific stimulation. $CD8^+$ T cells positively labeled with HLA-A*0201-$GAD65_{114–123}$ were FACS sorted at single cells into naive and memory T-cell subsets according to the expression of CD62L, CD45RA, and CD95. Single-sorted T-cell clones were stimulated in X-VIVO 15 (Lonza) supplemented with 5% inactivated FBS (Gibco) (culture medium) with HLA-A*0201-$GAD65_{114–123}$ dextramer (1 μg/mL) and anti-CD28 mAb (1 μg/mL; BD Biosciences) in the presence of 1,000 irradiated autologous monocytes for 7 days. After 7 days, half of the medium was replaced with fresh medium containing HLA-A*0201-$GAD65_{114–123}$ dextramer (1 μg/mL) and anti-CD28 mAb (2 μg/mL; BD Biosciences). The procedure was repeated a total of three times. The number of T cells in each well was determined at the end of the 4-week stimulation using an automated cell counter.

In Vitro Generation of GAD65-Specific Tscm From Naive Precursors

Peripheral blood mononuclear cells were isolated over a Ficoll Hypaque (Sigma-Aldrich) density gradient from sodium-heparinized venous blood samples. Highly purified (>97%) naive $CD8^+$ T cells were magnetically isolated using a Naive $CD8^+$ T Cell Isolation Kit (Miltenyi Biotec). Naive $CD8^+$ T cells (5×10^5/mL) were seeded in 96-well plates in culture medium and stimulated with HLA-A*0201-$GAD65_{114–123}$ dextramers (1 μg/mL) and anti-CD28 mAb (1 μg/mL; BD Biosciences) in the presence of irradiated autologous monocytes (5×10^5/mL) for 12 days. Cell cultures were supplemented or not with 10 ng/mL of rhIL-7 (R&D Systems).

T-Cell Bioenergetic Profile

Surrogate markers of oxidative phosphorylation and glycolysis were measured by flow cytometry using the following reagents according to the manufacturer's instructions. MitoTracker Green FM and MitoTracker Red FM were from Invitrogen-Molecular Probes. 2-(*N*-(7-nitrobenz-2-oxa-,1,3-diazol-4-yl)amino)-2-deoxyglucose (2NBDG) was from Life Technologies. L(+)lactate concentration was measured in the supernatants with a Lactate Assay Kit (Sigma-Aldrich).

Carboxyfluorescein Diacetate Succinimidyl Ester Proliferation Assay

Proliferation was determined using the carboxyfluorescein diacetate succinimidyl ester (CFSE; Molecular Probes) dilution assay as we previously described (9).

Confocal Microscopy

FACS-sorted GAD65-specific Tscm were generated from naive precursors, sorted, allowed to settle onto a 12-mm poly-L-lysine–coated coverslip (Biocoat; BD Pharmingen), and stained with CD3 AF594 (clone UCHT-1; BioLegend) and MitoTracker Green FM. Cells were subsequently fixed in 3% formaldehyde, permeabilized with methanol, and blocked in 0.25% fish skin gelatin. Proliferation of Tregs and T cells was visualized by 5-ethynyl-29-deoxyuridine (EdU) incorporation, according to the manufacturer's instructions (Click-It EdU; Invitrogen). All images were acquired with a Leica SP5 inverse laser scanning confocal microscope.

Statistical Analysis

Statistical analyses were performed using GraphPad Prism software. Flow cytometry data were calculated as mean fluorescence intensity (MFI) and subpopulations as percentage of positive cells. Proliferation was calculated as percentage of cells that diluted the fluorescent dye CFSE (%CFSEdim). Data were presented as mean and SD, and the Wilcoxon matched-pairs test was used for comparisons. A two-tailed P value <0.05 was considered significant. Comparison of GLUT1 and 2NBDG uptake was performed by linear regression analysis.

RESULTS

Detection of Circulating CD8$^+$ Tscm Specific for GAD65, Insulin, and IGRP in Patients With T1D

We measured CD8$^+$ T cells with a CD45RA$^+$CCR7$^+$CD95$^+$ Tscm phenotype within T cells specific for β-cell antigens GAD65, insulin, and IGRP identified by positive staining for HLA-A*0201 peptide dextramers in eight patients with LS-T1D, six patients with RO-T1D, and sex-matched subjects with no sign of autoimmunity (CTR) (Supplementary Tables 1 and 2). Patients with RO-T1D had an increased percentage (mean ± SD) of circulating Tscm specific for $GAD65_{114–123}$ (CTR 1.5 ± 1.2 vs. T1D 4.2 ± 2.1, $P = 0.0207$) and insulin $B_{10–18}$ (CTR 2.2 ± 2.6 vs. T1D 17.0 ± 7.4, $P = 0.015$) but a similar percentage of Tscm specific for $IGRP_{256–273}$ (CTR 2.3 ± 2.6 vs. T1D 6 ± 5.4, $P = 0.1667$) and influenza A $MP_{58–66}$ (CTR 9.4 ± 9.94 vs. T1D 12.11 ± 9.7, $P = 0.6545$) (Fig. 1*A* and *B*). Patients with LS-T1D had an increased percentage (mean ± SD) of circulating Tscm specific for $GAD65_{114–123}$ (CTR 2.7 ± 1.2 vs. T1D 15.6 ± 9.6, $P = 0.0021$), insulin $B_{10–18}$ (CTR 2.9 ± 1.9 vs. T1D 10.5 ± 6.1, $P = 0.0046$), and $IGRP_{256–273}$ (CTR 3.3 ± 2.1 vs. T1D 8.5 ± 4.8, $P = 0.1$) but a similar percentage of Tscm specific for influenza A $MP_{58–66}$ (CTR 14.8 ± 4.8 vs. T1D 14.3 ± 5, $P = 0.8414$). Overall, T cells specific for β-cell antigens were predominantly distributed among memory subsets in patients with T1D, whereas they showed a naive phenotype in CTR (Supplementary Table 3). The distribution of total CD8$^+$ T cells (Supplementary Fig. 1) was similar in patients with T1D and CTR. Patients with T1D also had an increased frequency of T-cell precursors specific for β-cell antigens but a similar frequency of T-cell precursors specific for influenza (Supplementary Fig. 2).

Autoreactive Tscm Preserve Telomere Length and Have a High Capacity for Clonal Expansion

In addition to the surface phenotype, we determined functional properties of Tscm, including telomere length and the potential for a single autoreactive Tscm clone to generate a clonal progeny (defined as clonal capacity). As a model of autoreactive T cells, we used ex vivo isolated $GAD65_{114–123}$–specific T cells from patients with T1D. Telomere length (MFI) was measured using a FITC-labeled PNA probe by flow cytometry as we previously described (9). Naive T cells (Tn) and Tscm have the longest telomeres, and there was not significant telomere shortening in the transition from Tn (1,827 ± 327) to Tscm (1,594 ± 163, $P = 0.14$). We observed a significant reduction of telomere length in Tcm (610 ± 131, $P = 0.017$), which was further reduced in Tem (394 ± 169, $P = 0.008$) and Temra (340 ± 117, $P = 0.008$) (Fig. 2*A* and *B*). To determine the clonal capacity, $GAD65_{114–123}$–specific T cells were FACS sorted at single cell and restimulated with $GAD65_{114–123}$ dextramers, anti-CD28, and autologous monocytes for 4 weeks. We subsequently counted the number of progenitor T cells (where present) and the T-cell subset distribution by phenotypic analysis. With respect to expansion, we considered both the percentage of single T-cell clones that generated a progeny of at least 100 cells (% responders) and the absolute number of T cells generated by each expanding clone (cells/well). Tscm (77% responders, 3,306 ± 2,609) showed a superior capacity for clonal expansion compared with Tn (30% responders, 1,411 ± 1,135, $P = 0.015$), Tcm (34%, 1,693 ± 1,020, $P = 0.045$), Tem (20%, 606 ± 520, $P = 0.038$), and Temra (17%, 411 ± 228, $P = 0.031$) (Fig. 2*C*). We performed a phenotypic analysis of expanded cells to characterize the T-cell subsets in the progeny and to determine whether after expansion there were cells retaining a Tscm phenotype. T cells expanded from single Tn clones generated a progeny distributed in memory subsets with 30% of cells still retaining a naive phenotype and 1.5% with a Tscm phenotype (Fig. 2*D*). Tscm differentiated mostly in memory subsets, and the percentage of cells retaining a Tscm phenotype was ∼6%. Tcm and Tem generated only memory cells with no detectable Tscm in the progeny. Temra were not analyzed for insufficient cell yield after expansion.

IL-7 Signaling Promotes the Generation of Autoreactive CD8$^+$ Tscm

Tscm can be generated by activation of naive precursors with antigen in the presence of homeostatic cytokines IL-7 and IL-15 (12). Sorted CD8$^+$CD45RA$^+$CD62L$^+$CD95$^-$ naive T cells were activated and expanded by incubation with $GAD65_{114–123}$ dextramers, anti-CD28 mAb, and autologous monocytes with or without 10 ng/mL IL-7 for 15 days. GAD65-specific T cells were identified postexpansion by dextramer staining (Fig. 3*A*) and analyzed. Sorted dextramer-positive T cells retained antigen specificity after expansion (Supplementary Fig. 3). The addition of IL-7 resulted in an increased frequency (percentage) of GAD65-specific T-cell clones (medium 3.97 ± 2.68 vs. IL-7 7.07 ± 1.83, $P = 0.0417$) (Fig. 3*A*). The GAD65-specific progeny was studied for phenotype, telomere length, and clonal capacity. The frequency of Tscm was significantly higher in the presence of IL-7 (medium 3.13 ± 1.39 vs. IL-7 23.50 ± 9.98, $P = 0.006$) (Fig. 3*B*). With respect to telomere length (MFI), we found no significant differences in Tscm generated in the presence or absence of IL-7 (medium 1,520 ± 367 vs. IL-7 1,758 ± 419, $P = 0.2072$) (Fig. 3*C*). Also, the clonal capacity was not significantly different in Tscm generated with or without IL-7 (medium: 75% responders [8,019 ± 9,540] vs. IL-7: 85% responders [11,550 ± 12,762]; $P = 0.3877$) (Fig. 3*D*).

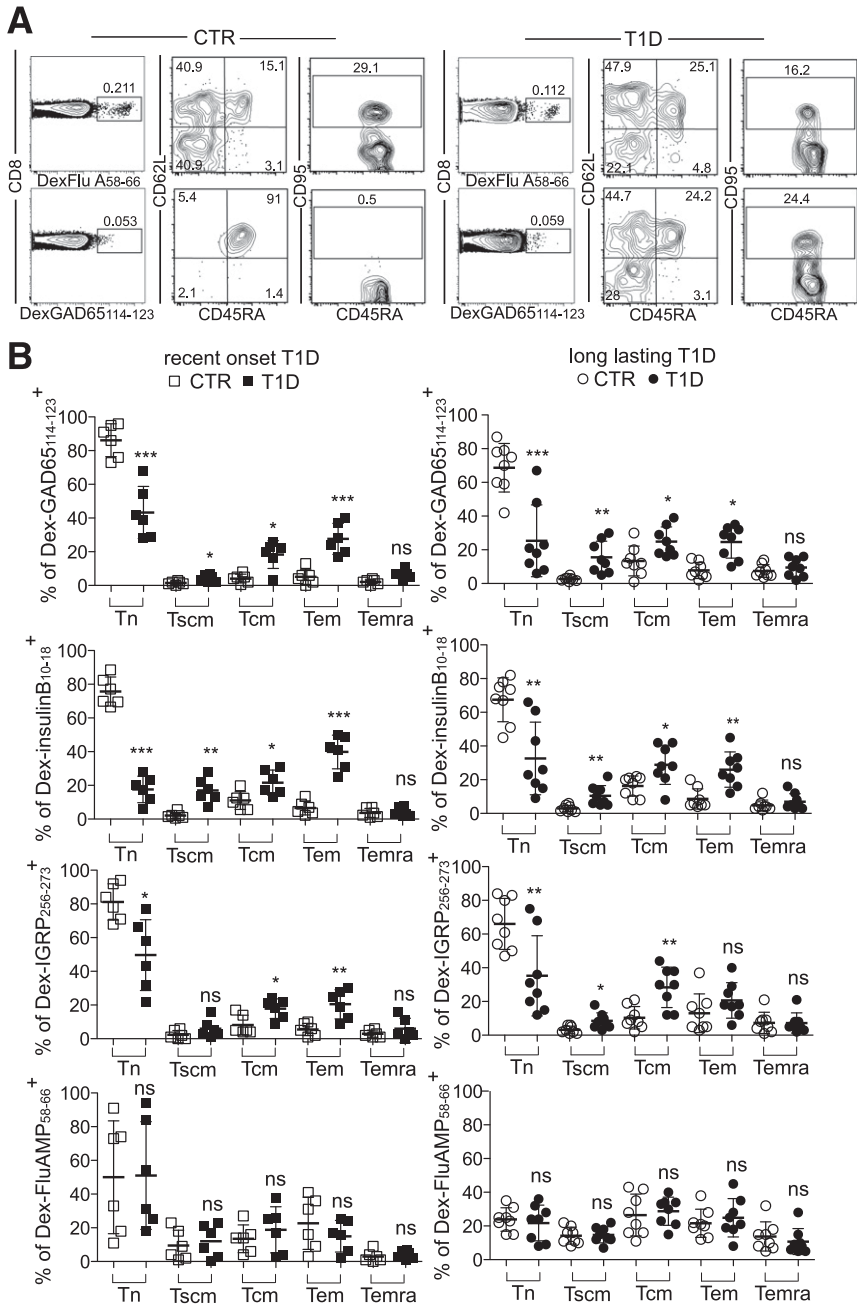

Figure 1—Autoreactive Tscm are present in patients with T1D. *A*: FACS plots show gating of $CD8^+$dextramer$^+$ T cells (left) with a $CD45RA^+CCR7^+$ phenotype (center) and the $CD95^+$ Tscm population (right). Plot shows a control subject (CTR, left) and a patient with T1D (T1D, right). *B*: Graphs show how dextramer$^+$ T cells are distributed in the Tn, Tcm, Tem, Temra, and Tscm subsets in T cells specific for $GAD65_{114–123}$, insulin $B_{10–18}$, $IGRP_{256–273}$, and influenza A $MP_{58–66}$. Graphs show control subjects (□, $n = 6$), patients with RO-T1D (■, $n = 6$), control subjects (○, $n = 8$), and patients with LS-T1D (●, $n = 8$). $^*P < 0.05$; $^{**}P < 0.01$; $^{***}P < 0.001$.

IL-7 Induces Metabolic Changes in Differentiating Naive T Cells

IL-7 is known to affect bioenergetic metabolism of T cells, including upregulation of GLUT1 to promote glycolysis. Therefore, we investigated the metabolic signature of naive precursors stimulated with GAD65 in the absence or presence of IL-7. First, we determined GLUT1 expression in the progeny of GAD65-specific Tn from patients with T1D expanded in the absence or presence of IL-7. We found that GLUT1 was overexpressed (MFI) in Tscm as compared with Tn, Tcm, and Tem and was further upregulated by IL-7 (medium 490 ± 91 vs. IL-7 685 ± 108, $P = 0.0069$) (Fig. 4*A*). Corroborating these findings, an increase of the key glycolytic enzyme hexokinase 2 (HK2) was found after 12 h of stimulation of Tn with IL-7 (Fig. 4*B*). The expression of key enzymes of mitochondrial respiration (carnitine palmitoyltransferase 1A, cytochrome c oxidase subunit 6A1, and ATP synthase subunit α), glutaminolysis (glutaminase 2),

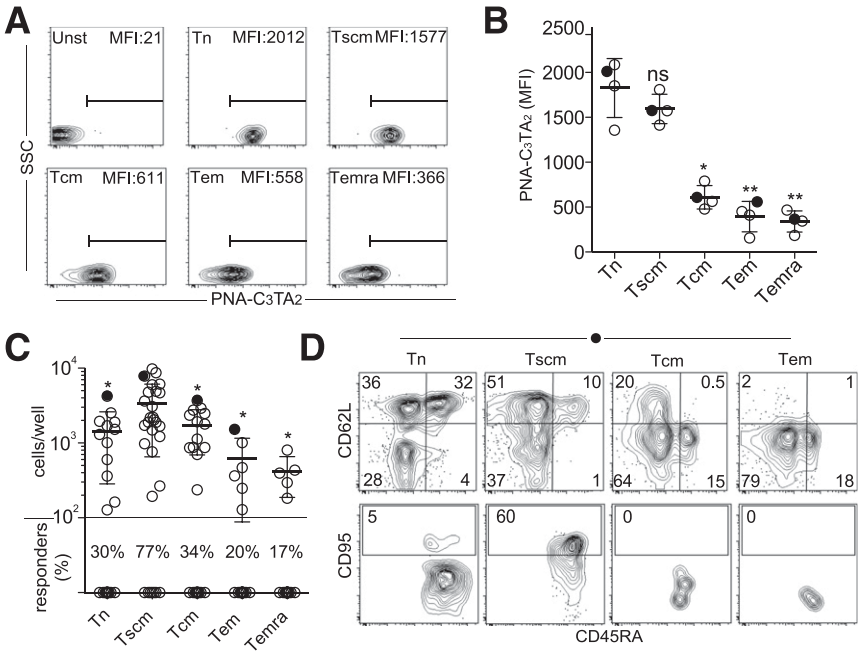

Figure 2—Telomere length and clonal capacity of ex vivo isolated $GAD65_{114–123}$ T-cell clones. *A*: FACS plots showing telomere probe fluorescence of T-cell subsets from sorted $GAD65_{114–123}$–specific T cells. Plots are represented as side scatter (SSC) vs. PNA probe fluorescence. An unstained (Unst) sample is shown in the upper-left plot. The MFI is indicated in the upper-right corner of each plot. *B*: Telomere length of T-cell subsets from $GAD65_{114–123}$–specific T cells obtained from four different patients with T1D. Open circles (○) indicate each individual sample and filled circles (●) indicate the sample shown in *A*. *C*: Graph shows the clonal capacity of single $GAD65_{114–123}$–specific T cells sorted as T-cell subsets. Both the percentage of clones that expanded (% responders) and the absolute number of cells of clones that expanded (cells/well) are indicated in the graph. *D*: Phenotype (CD45RA, CD62L, and CD95) of the progeny from single-cell clone (●) from *C*. ns, not significant. $^*P = 0.05$; $^{**}P = 0.01$.

and glycolysis (phosphoglycerate kinase 1 and glucose-6-phosphate dehydrogenase) was not affected by the presence of IL-7. Based on these results, we sought to determine the basal metabolic signature of Tscm specific for GAD65 and influenza (as control) generated with or without IL-7. Due to the low cell numbers available in the antigen-specific context, we used surrogate metabolic markers for flow cytometry and measured lactate in the culture supernatants. With respect to flow cytometry, we measured the uptake of the fluorescent glucose analog 2NBDG, the mitochondrial cell mass with the MitoGreen dye, and the mitochondrial activity with the MitoRed dye (Fig. 4*C*). GAD65-specific Tscm generated in the presence of IL-7 had increased glucose uptake (medium 855 ± 476 vs. IL-7 1,827 ± 596, P = 0.0109) but similar lactate production (mmol/mL; medium 281 ± 99 vs. IL-7 300 ± 79, P = 0.7581) and increased mitochondrial mass (medium 5,078 ± 1,644 vs. IL-7 10,441 ± 3,237, P = 0.0047) and activity (medium 2,196 ± 604 vs. IL-7 3,072 ± 647, P = 0.0359). A similar metabolic signature was found in influenza-specific T cells, indicating that this metabolic profile is not confined to autoreactive T cells. Corroborating these findings, proliferating Tn cultured in the presence of IL-7 for 72 h showed a high mitochondrial cell mass in confocal microscopy (Fig. 4*D*). We subsequently determined the metabolic signature of circulating $CD8^+$ T-cell subsets in patients with T1D and CTR. Metabolic markers, including the mitochondrial mass, activity, and glucose uptake, were similar among circulating T-cell subsets and were similar in T1D compared with CTR, indicating that the metabolic dysregulation of T1D and insulin therapy does not directly impact the basal metabolism of resting circulating T cells (Supplementary Fig. 4). However, GLUT1 was overexpressed (as MFI) in circulating Tscm as compared with the other T-cell subsets (Fig. 4*E*), and less differentiated Tn, Tscm, and Tcm have a higher percentage of $GLUT1^+$ cells (Supplementary Fig. 5). We found a direct correlation between GLUT1 expression and the uptake of 2NBDG (Fig. 4*F*), suggesting that GLUT1 is an important GLUT in T cells in vivo. To determine the importance of glucose metabolism in T-cell subsets, Tn, Tscm, Tcm, and Tem were activated by polyclonal stimulation with anti-CD3/CD28 in the presence of different concentrations of glucose. Cell division was predominantly affected in Tscm (Fig. 4*G*), showing the dependence of Tscm from the availability of extracellular glucose. Overexpression of GLUT1 was confirmed in circulating GAD65- and influenza-specific Tscm from patients with T1D (Fig. 4*H*).

Metabolic Targeting of Tscm

Our findings suggested that Tscm metabolism relies on glucose for the generation of pyruvate that can be subsequently transported to and oxidized in the mitochondria. Therefore, we tested the GLUT1 inhibitor WZB117 (18) and the mitochondrial pyruvate transporter inhibitor UK5099 (19) for metabolic manipulation of Tscm. We chose a WZB117

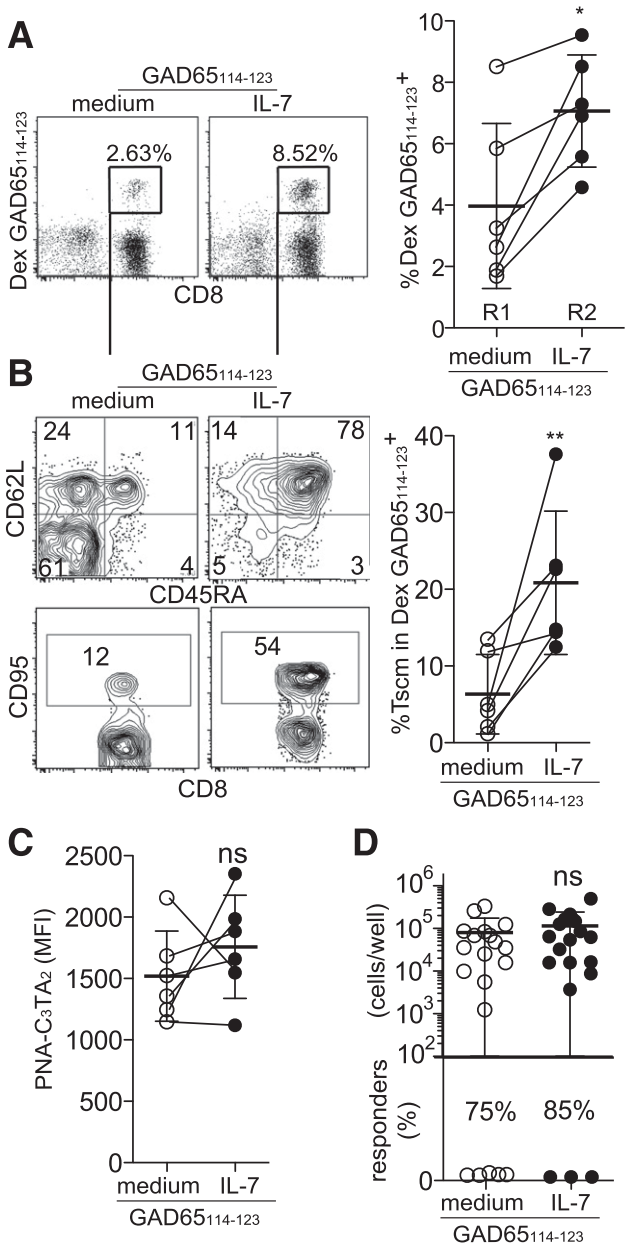

Figure 3—Generation of GAD65-specific Tscm from naive precursors. *A*: FACS plot (left) showing the frequency of GAD65-specific T cells after 15 days of expansion of $GAD65_{114–123}$–specific Tn precursors. Graph shows the results from six different subjects with T1D. Open circles (○) indicate cells stimulated with medium only, and filled circles (●) indicate cells stimulated with IL-7. *B*: FACS plot (left) showing the phenotype (CD45RA, CD62L, and CD95) of T cells after 15 days of expansion with $GAD65_{114–123}$ in the presence or absence of IL-7. Right graph shows the results from six different subjects. Telomere length of in vitro generated GAD65-specific Tscm in the presence or absence of IL-7. *C*: Telomere length of in vitro GAD65-specific T cells generated in the presence or absence of IL-7. *D*: Clonal capacity of in vitro GAD65-specific T cells generated in the presence or absence of IL-7. ns, not significant. $^*P = 0.05$; $^{**}P = 0.01$.

concentration of 3 μmol/L, which resulted in a 75% inhibition of glucose uptake, and UK5099 at 10 μmol/L, which resulted in a 75% upregulation of lactate production in Tn stimulated with IL-7. We next determined the effect of WZB117 and UK5099 in our in vitro model of differentiation of GAD65-specific Tn in the presence of IL-7 (Fig. 5*A*). Both WZB117 and UK5099 selectively reduced the differentiation of Tscm (medium 12.9 ± 2.5 vs. WZB117 6.1 ± 2.5 vs. UK5099 5.8 ± 2.3) without a significant effect on the differentiation of other T-cell subsets (Supplementary Fig. 6). Then we determined the effect of WZB117 and UK5099 on GAD65-specific Tscm division and apoptosis using a CFSE dilution assay and 7AAD staining. WZB117 strongly suppressed Tscm division (Fig. 5*C*) without causing significant apoptosis (Supplementary Fig. 7). Conversely, UK5099 did not prevent cell division but induced a high rate of apoptosis. When used in combination, we observed a dominant effect of WZB117. Both WZB117 and UK5099 minimally affected proliferation and apoptosis in Tcm.

DISCUSSION

The T-cell repertoire, including the presence of autoreactive T-cell clones, is determined early in life in patients with T1D, but the differentiation into pathogenic memory clonal populations occurs later as a consequence of antigen encounter and homeostatic mechanism involving IL-7 (20). By examining in vivo T cells, we were able to identify circulating autoreactive T cells with a Tscm phenotype and properties. We determined the mechanism for their generation from naive precursors and identified pathways that are potential therapeutic targets to control Tscm generation and expansion. These findings are relevant to understanding the pathogenesis of autoimmunity and to find ways to control the autoimmune response in patients with T1D.

The presence of a memory response to islet autoantigens can be associated with the limited success of immunotherapies tested thus far in patients with T1D. Naive T cells reactive to β-cell antigens are already detectable at birth (20), preprimed in infancy before the appearance of memory T cells (21), and acquire memory phenotype and function before the onset of the disease (9). Autoimmune memory is then maintained for decades after the disease onset, as testified in patients with T1D receiving islet or pancreas transplants, which despite immunosuppression, can be associated with reactivation of autoimmunity (22). Memory autoimmunity is highly refractory to modulation with immunosuppressive drugs and immune-modulating molecules (15, 23), mostly designed to target activated and rapidly proliferating effector T cells. These raised the question of whether resistant and long-lived autoreactive Tscm precursors can act as a reservoir of autoreactive clones in autoimmunity relapse after treatment (6). The identification of circulating Tscm specific for GAD65, insulin, and IGRP supports this hypothesis but also provides a novel target cell population to design innovative immunotherapy approaches. A selective targeting of autoreactive Tscm clones can be adopted to permanently delete the more differentiated T-cell progeny. This approach is similar in principle to that hypothesized to treat cancer by targeting cancer stem cells (24). In this theory, a permanent eradication of a tumor mass can

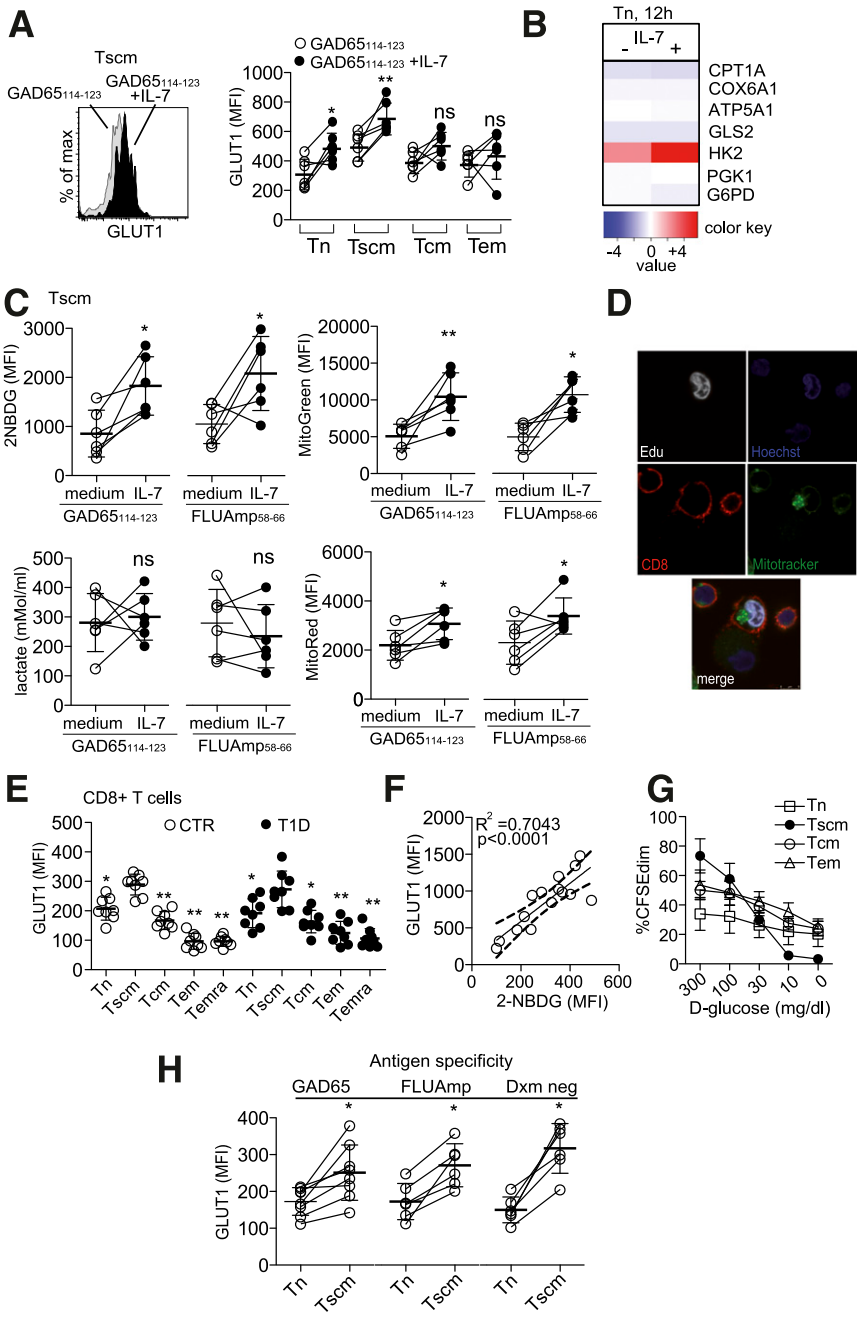

Figure 4—Metabolic signature of GAD65-specific Tscm generated in the presence or absence of IL-7. *A*: GLUT1 expression in T-cell subsets generated from Tn precursors from patients with T1D in the presence or absence of IL-7. *B*: Expression of enzymes of the glycolytic pathway (HK2, PGK1, and G6PD), glutaminolysis (GLS2), and mitochondrial respiration (CPT1A, COX6A1, and ATP5A1) in CD8$^+$ naive T cells stimulated for 12 h with IL-7. *C*: Uptake of 2NBDG, lactate production, mitochondrial mass, and mitochondrial activity of GAD65- and influenza-specific Tscm generated from naive precursors in the presence or absence of IL-7. *D*: Confocal microscopy image showing the mitochondrial mass (MitoTracker) of a proliferating (EdU positive) CD8$^+$ T cell stimulated with GAD65 in the presence of IL-7. *E*: Expression of GLUT1 in circulating CD8$^+$ T-cell subsets from patients with T1D and CTR. *F*: Correlation of GLUT-1 expression and 2NBDG uptake in ex vivo CD8$^+$ T cells from patients with T1D. *G*: CFSE dilution assay of Tn, Tscm, Tcm, and Tem stimulated with anti-CD3/CD28 in the presence of increasing concentrations of D-glucose. *H*: FACS plot showing the expression of GLUT1 in circulating GAD65- and influenza-specific and dextramer-negative Tscm from six patients with T1D. ns, not significant. *P = 0.05; **P = 0.01.

be achieved by selective targeting of rare and slowly proliferating cancer stem cell precursors. In contrast, standard radiochemotherapy targeting the rapidly proliferating cancer cells, but not cancer stem cells, results in a high rate of tumor relapse.

To determine molecular determinants in the generation of autoreactive Tscm from naive precursors, we set up in vitro models in which Tscm are generated under the influence of IL-7. Differentiation of a large number of Tscm was successfully set up by culturing naive T-cell precursors

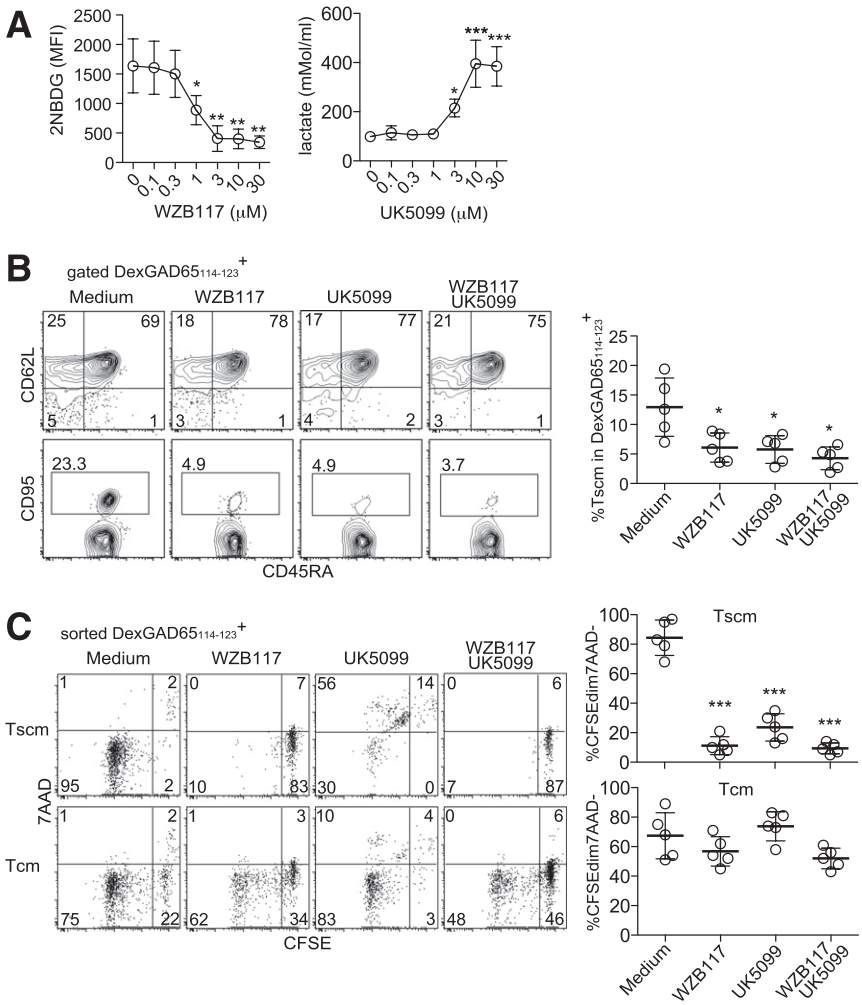

Figure 5—Metabolic targeting of Tscm with WZB117 and UK5099. *A*: Dose-response effect of WZB117 on 2NBDG uptake and of UK5099 on lactate production in Tn cultured with IL-7. *B*: FACS plots show the percentage of Tscm generated from Tn precursors in the presence of WZB117 and UK5099 alone or in combination. Graph on the right shows a summary of five experiments. *C*: FACS plots show a CFSE dilution assay and 7AAD staining of sorted GAD65-specific Tscm and Tcm in the presence of WZB117 and UK5099 alone or in combination. Graphs show the results from five different experiments. ns, not significant. **P* = 0.05; ***P* = 0.01; ****P* = 0.001.

with anti-CD3/CD28 in the presence of IL-7 and IL-15 (12). In our system of antigen-specific stimulation with GAD65 (as a model autoantigen), we preferred to use only IL-7 as the addition of IL-15 was associated with non–antigen-specific proliferation. Tscm generated with IL-7 displayed three fundamental Tscm characteristics: a $CD45RA^+CD62L^+CD95^+$ phenotype, high clonal capacity, and preservation of telomere length. Tscm with similar characteristics were also generated by stimulation with GAD65 only; however, the presence of IL-7 strongly increased the frequency of Tscm. Moreover, IL-7 is highly relevant to the pathogenesis of T1D. IL-7 accelerates diabetes onset in the nonobese diabetic mouse (25), whereas blockade of IL-7R can reverse diabetes in the same model (26, 27). In humans, single nucleotide polymorphisms of IL-7Rα are associated with an increased risk for developing T1D (28), and dysregulation of the IL-7/IL-7R axis was proposed in patients with diagnosed T1D (29). We also showed that IL-7 is elevated post–islet transplantation, boosting autoreactive memory T-cell expansion (30). This is relevant to the presence of pretransplant autoreactive Tscm as supraphysiological levels of IL-7 posttransplant can potentially activate these cells and trigger recurrence of autoimmunity to affect islet graft survival. Further studies are needed to address whether the frequency of autoreactive Tscm pretransplant and the posttransplant levels of IL-7 are predictive biomarkers of autoimmunity recurrence.

Therefore, the generation of a high number of autoreactive Tscm by IL-7 can represent a potential novel link between the IL-7/IL-7 receptor axis and the development of T-cell responses toward β-cells. Tscm generation under the influence of IL-7 was related to glucose uptake via GLUT1, in line with previous observations (31). However, the production of lactate was similar to that of cells generated in the absence of IL-7, suggesting a similar rate of anaerobic glycolysis. Moreover, both the mitochondrial cell mass and activity were increased by IL-7. An interesting possibility was that glucose is transformed in pyruvate that is subsequently transported in mitochondria for oxidation. This was further

supported by the effect of the mitochondria pyruvate transporter inhibitor UK5099, which reduced proliferation and differentiation of Tscm. This metabolic signature is different from the aerobic glycolysis that is strongly activated in proliferating effector T cells and is more similar to the oxidative metabolism described in memory subsets, including Tscm and Tcm (32). Importantly, glucose is a preferred substrate for long-lived cells such as neurons (33) and hematopoietic stem cells residing in hypoxic niches of the bone marrow (34). A possible reason for the use of glucose can be to limit the accumulation of reactive oxygen species that can damage cell structures such as membrane lipids and DNA (35). In circulating Tscm from patients (in which cells are in the resting state), we were not able to determine differences in the bioenergetic metabolism. However, we observed substantial differences with respect to the surface expression of GLUT1. Aiming to identify a novel target pathway for inhibition of Tscm, we focused our study on targeting glucose metabolism by inhibiting GLUT1 or the mitochondrial pyruvate transporter. Several inhibitors of glycolysis have been developed and tested in clinical trials in cancer research, showing significant toxicity (36). A novel class of small molecules described as selective inhibitors of GLUT1 have been recently described and proven effective in the inhibition of cancer cell lines in mouse models (18). Of these, WZB117 appeared to be more selective for GLUT1 and was selected for our study. Although the mitochondrial pyruvate transporter inhibitor UK5099 was useful to demonstrate the importance of pyruvate oxidation in the mitochondria, WZB117 showed a dominant effect in the generation and inhibition of Tscm and is therefore a promising candidate molecule for further testing in animal models. With respect to potential side effects of GLUT1 inhibition in humans, studies of the GLUT1 deficiency syndrome reported mild to severe neurological disorders in infants and children affected, whereas in adult life, most symptoms were stable or diminished (37). Since overexpression of GLUT1 is not limited to autoreactive T cells and metabolism is increased in activated T cells, we can envisage a strategy in which adult patients undergoing islet transplantation have a selective reactivation of autoreactive T-cell clones (38). This model provides the opportunity for using WZB117 for a limited time period and increasing the selectivity of the treatment for activated autoreactive T cells that upregulate glucose uptake.

Our study provides key insight into the potential role of long-lived autoreactive Tscm in β-cell autoimmunity as a reservoir of pathogenetic effector T cells in the relapse of autoimmunity after immunotherapy or islet transplantation. Second, expression of GLUT1 may be used as a target to selectively inhibit autoreactive Tscm generation and expansion upon antigen-specific activation.

Funding. This work was supported by the Italian Ministry of Health (RF-2009-1469691) and the European Foundation for the Study of Diabetes/JDRF/Novo Nordisk Programme. P.M. is supported by a Career Development Award from JDRF (5-CDA-2015-85-A-N).

Duality of Interest. This work was supported by Becton Dickinson. No other potential conflicts of interest relevant to this article were reported.

Author Contributions. D.V. designed and performed the experiments, analyzed data, and contributed to the writing of the manuscript. E.C., C.B., A.Ca., and A.Ci. set up and performed the experiments. A.A. supervised the experiments in the animal model and analyzed data. L.P. and P.M. designed the study, supervised the work, analyzed data, and wrote the manuscript. P.M. is the guarantor of this work and, as such, had full access to all the data in the study and takes responsibility for the integrity of the data and the accuracy of the data analysis.

References

1. Sallusto F, Geginat J, Lanzavecchia A. Central memory and effector memory T cell subsets: function, generation, and maintenance. Annu Rev Immunol 2004;22:745–763
2. Vrisekoop N, den Braber I, de Boer AB, et al. Sparse production but preferential incorporation of recently produced naive T cells in the human peripheral pool. Proc Natl Acad Sci U S A 2008;105:6115–6120
3. Gattinoni L, Zhong X-S, Palmer DC, et al. Wnt signaling arrests effector T cell differentiation and generates CD8+ memory stem cells. Nat Med 2009;15:808–813
4. Lugli E, Dominguez MH, Gattinoni L, et al. Superior T memory stem cell persistence supports long-lived T cell memory. J Clin Invest 2013;123:594–599
5. Gattinoni L, Lugli E, Ji Y, et al. A human memory T cell subset with stem cell-like properties. Nat Med 2011;17:1290–1297
6. Monti P, Heninger AK, Bonifacio E. Differentiation, expansion, and homeostasis of autoreactive T cells in type 1 diabetes mellitus. Curr Diab Rep 2009;9:113–118
7. Di Lorenzo TP, Peakman M, Roep BO. Translational mini-review series on type 1 diabetes: systematic analysis of T cell epitopes in autoimmune diabetes. Clin Exp Immunol 2007;148:1–16
8. Danke NA, Yang J, Greenbaum C, Kwok WW. Comparative study of GAD65-specific CD4+ T cells in healthy and type 1 diabetic subjects. J Autoimmun 2005;25:303–311
9. Monti P, Scirpoli M, Rigamonti A, et al. Evidence for in vivo primed and expanded autoreactive T cells as a specific feature of patients with type 1 diabetes. J Immunol 2007;179:5785–5792
10. Viglietta V, Kent SC, Orban T, Hafler DA. GAD65-reactive T cells are activated in patients with autoimmune type 1a diabetes. J Clin Invest 2002;109:895–903
11. Monti P, Bonifacio E. Interleukin-7 and type 1 diabetes. Curr Diab Rep 2014;14:518–524
12. Cieri N, Camisa B, Cocchiarella F, et al. IL-7 and IL-15 instruct the generation of human memory stem T cells from naive precursors. Blood 2013;121:573–584
13. Huurman VA, Hilbrands R, Pinkse GG, et al. Cellular islet autoimmunity associates with clinical outcome of islet cell transplantation. PLoS One 2008;3:e2435
14. Orban T, Bundy B, Becker DJ, et al.; Type 1 Diabetes TrialNet Abatacept Study Group. Co-stimulation modulation with abatacept in patients with recent-onset type 1 diabetes: a randomised, double-blind, placebo-controlled trial. Lancet 2011;378:412–419
15. Sherry N, Hagopian W, Ludvigsson J, et al.; Protégé Trial Investigators. Teplizumab for treatment of type 1 diabetes (Protégé study): 1-year results from a randomised, placebo-controlled trial. Lancet 2011;378:487–497
16. Wherrett DK, Bundy B, Becker DJ, et al.; Type 1 Diabetes TrialNet GAD Study Group. Antigen-based therapy with glutamic acid decarboxylase (GAD) vaccine in patients with recent-onset type 1 diabetes: a randomised double-blind trial. Lancet 2011;378:319–327
17. Malmegrim KC, de Azevedo JT, Arruda LC, et al. Immunological balance is associated with clinical outcome after autologous hematopoietic stem cell transplantation in type 1 diabetes. Front Immunol 2017;8:167
18. Liu Y, Cao Y, Zhang W, et al. A small-molecule inhibitor of glucose transporter 1 downregulates glycolysis, induces cell-cycle arrest, and inhibits cancer cell growth in vitro and in vivo. Mol Cancer Ther 2012;11:1672–1682
19. Zhong Y, Li X, Yu D, et al. Application of mitochondrial pyruvate carrier blocker UK5099 creates metabolic reprogram and greater stem-like properties in LnCap prostate cancer cells in vitro. Oncotarget 2015;6:37758–37769

20. Heninger AK, Monti P, Wilhelm C, et al. Activation of islet autoreactive naïve T cells in infants is influenced by homeostatic mechanisms and antigen-presenting capacity. Diabetes 2013;62:2059–2066
21. Heninger AK, Eugster A, Kuehn D, et al. A divergent population of autoantigen-responsive CD4+ T cells in infants prior to β cell autoimmunity. Sci Transl Med 2017;9:pii:eaaf8848
22. Roep BO, Stobbe I, Duinkerken G, et al. Auto- and alloimmune reactivity to human islet allografts transplanted into type 1 diabetic patients. Diabetes 1999; 48:484–490
23. Monti P, Brigatti C, Heninger AK, Scirpoli M, Bonifacio E. Disengaging the IL-2 receptor with daclizumab enhances IL-7-mediated proliferation of CD4(+) and CD8(+) T cells. Am J Transplant 2009;9:2727–2735
24. Beck B, Blanpain C. Unravelling cancer stem cell potential. Nat Rev Cancer 2013;13:727–738
25. Calzascia T, Pellegrini M, Lin A, et al. CD4 T cells, lymphopenia, and IL-7 in a multistep pathway to autoimmunity. Proc Natl Acad Sci U S A 2008;105: 2999–3004
26. Lee LF, Logronio K, Tu GH, et al. Anti-IL-7 receptor-α reverses established type 1 diabetes in nonobese diabetic mice by modulating effector T-cell function. Proc Natl Acad Sci U S A 2012;109:12674–12679
27. Penaranda C, Kuswanto W, Hofmann J, et al. IL-7 receptor blockade reverses autoimmune diabetes by promoting inhibition of effector/memory T cells. Proc Natl Acad Sci U S A 2012;109:12668–12673
28. Todd JA, Walker NM, Cooper JD, et al.; Genetics of Type 1 Diabetes in Finland; Wellcome Trust Case Control Consortium. Robust associations of four new chromosome regions from genome-wide analyses of type 1 diabetes. Nat Genet 2007;39: 857–864
29. Monti P, Brigatti C, Krasmann M, Ziegler AG, Bonifacio E. Concentration and activity of the soluble form of the interleukin-7 receptor α in type 1 diabetes identifies an interplay between hyperglycemia and immune function. Diabetes 2013;62:2500–2508
30. Monti P, Scirpoli M, Maffi P, et al. Islet transplantation in patients with autoimmune diabetes induces homeostatic cytokines that expand autoreactive memory T cells. J Clin Invest 2008;118:1806–1814
31. Wofford JA, Wieman HL, Jacobs SR, Zhao Y, Rathmell JC. IL-7 promotes Glut1 trafficking and glucose uptake via STAT5-mediated activation of Akt to support T-cell survival. Blood 2008;111:2101–2111
32. Pearce EL. Metabolism in T cell activation and differentiation. Curr Opin Immunol 2010;22:314–320
33. Mergenthaler P, Lindauer U, Dienel GA, Meisel A. Sugar for the brain: the role of glucose in physiological and pathological brain function. Trends Neurosci 2013;36: 587–597
34. Simsek T, Kocabas F, Zheng J, et al. The distinct metabolic profile of hematopoietic stem cells reflects their location in a hypoxic niche. Cell Stem Cell 2010;7: 380–390
35. Belikov AV, Schraven B, Simeoni L. T cells and reactive oxygen species. J Biomed Sci 2015;22:85–92
36. Chang C-H, Curtis JD, Maggi LB Jr, et al. Posttranscriptional control of T cell effector function by aerobic glycolysis. Cell 2013;153:1239–1251
37. Leen WG, Taher M, Verbeek MM, Kamsteeg EJ, van de Warrenburg BP, Willemsen MA. GLUT1 deficiency syndrome into adulthood: a follow-up study. J Neurol 2014;261:589–599
38. Bordignon C, Canu A, Dyczko A, Leone S, Monti P. T-cell metabolism as a target to control autoreactive T cells in β-cell autoimmunity. Curr Diab Rep 2017;17:24